Science of the Total Environment 665 (2019) 620–631

Contents lists available at ScienceDirect

Science of the Total Environment

journal homepage: www.elsevier.com/locate/scitotenv

Contrasting wheat phenological responses to climate change in global scale

Shilong Ren, Qiming Qin *, Huazhong Ren

Institute of Remote Sensing and Geographic Information System, School of Earth and Space Sciences, Peking University, Beijing 100871, PR China

HIGHLIGHTS

- Three wheat phenology estimation methods were compared in this study.
- Air temperature mainly determines the spatiotemporal patterns of wheat phenology.
- Precipitation only exhibited a strong impact on growing season peak and end.
- Growing season start and peak were also closely connected with frost frequency.
- An opposite impact of haze weather on wheat phenology was found in China and India.

GRAPHICAL ABSTRACT

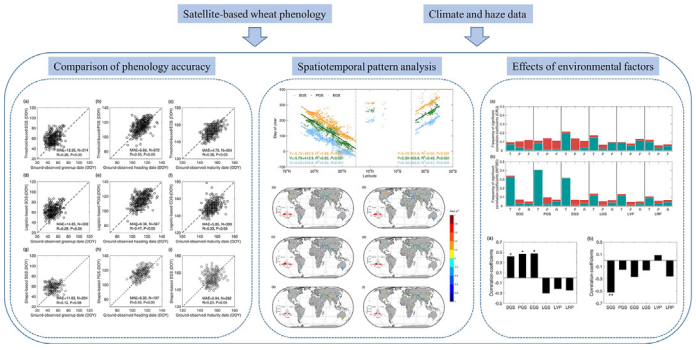

ARTICLE INFO

Article history:
Received 6 December 2018
Received in revised form 28 January 2019
Accepted 29 January 2019
Available online 30 January 2019

Editor: Elena Paoletti

Keywords:
Wheat phenology
Spatiotemporal pattern
Temperature
Precipitation
Haze
Frost

ABSTRACT

Comprehensive analysis of how wheat phenology responds to environmental factors in global scale is helpful for tackling the possible adverse effects of ongoing climate change on wheat production. In this study, six phenological parameters of global wheat, i.e., the growing season start (SGS), peak (PGS), end (EGS), length (LGS), as well as the vegetative period length (LVP) and reproductive period length (LRP), were retrieved from remote sensing data (1981–2014) by threshold-, logistic-, and shape-based methods. And then, we analyzed the effects of temperature, precipitation, short-wave (SW) radiation, and frost on spatiotemporal patterns of wheat phenology. In addition, haze impacts on wheat phenology were investigated in China and India where haze weather appears frequently in winter-spring seasons. Results showed that the occurrence time of SGS/PGS/EGS is gradually advanced from the pole to the equator and annual mean air temperature can explain >70% of their spatial variations. A dominant advanced SGS/PGS/EGS and a shortened LGS/LVP/LRP were detected in the study region due to the significant increase in temperature and SW radiation, as well as the decrease in frost days. Interannual fluctuations of SGS/PGS/EGS are primarily controlled by air temperature, while precipitation and frost only exerted some obvious impacts in some locations. Higher preseason temperature would induce an earlier wheat phenology and a shorter growing season, while adequate precipitation and frequent frost in preseason could delay the occurrence timing of wheat phenology and lead to a longer growing season. Besides, the decreased temperature resulted from severe haze weather may have partly counteracted the global-warming-induced advancing trend of wheat phenology in China, but further advanced the occurrence timing of wheat phenology through prompting vernalization in India. Overall, though wheat growth is largely constrained by human management, we still highlight the strong impacts of global climate change on wheat phenology.

© 2019 Elsevier B.V. All rights reserved.

* Corresponding author.
E-mail addresses: renshilong@pku.edu.cn (S. Ren), qmqin@pku.edu.cn (Q. Qin), renhuazhong@pku.edu.cn (H. Ren).

https://doi.org/10.1016/j.scitotenv.2019.01.394
0048-9697/© 2019 Elsevier B.V. All rights reserved.

1. Introduction

Over the past several decades, vegetation phenology has attracted a lot of attention within the context of global climate change, not only because it can effectively serve as an important indicator of climate change (Cleland et al., 2006; Penuelas et al., 2009; Richardson et al., 2013), but also due to its strong effects on terrestrial carbon budget and ecosystem productivity (Piao et al., 2008; Richardson et al., 2013). However, most studies have thus far focused on the phenological changes of natural vegetation and only a few have dealt with the phenological trends of agricultural varieties (Estrella et al., 2009; Hu et al., 2005; Siebert and Ewert, 2012; Tao et al., 2006). Since cultivated land accounts for about 12% of the global land area (Ramankutty and Foley, 1998), phenological changes in crops greatly affect global terrestrial material and energy exchange and crop yields (Asseng et al., 2015; Lokupitiya et al., 2009).

Among the common crops, wheat is the most widely grown in the world and has raised >35% of the world's population. Based on long-term ground records, many studies have detected a significant advance in wheat phenology (such as the date of shooting, heading, yellow ripeness, and harvest) over the past several decades in Germany (Estrella et al., 2007), the U.S. Great Plains (Hu et al., 2005), and China (Liu et al., 2018; Tao et al., 2006; Xiao et al., 2015), with the changing rate from 0.1 days yr^{-1} to 0.31 days yr^{-1}. Simultaneously, the lengths of the entire and vegetative growing periods have significantly reduced, while the length of the reproductive growing period has significantly increased (Tao et al., 2006). All these shifts were primarily attributed to the significant increase of the preseason or in-season temperature (Estrella et al., 2007; Lobell et al., 2012). Sunshine duration is another critical key in regulating the development rate of wheat during the vegetative period, which is usually calculated from the day of the year and latitude using standard astronomical equations (Sadras and Monzon, 2006). However, sunshine duration is actually not a constant for a specific day of year in a location due to the effects of weather (Matuszko, 2012). Besides, phenological shifts induced by temperature variation would influence the effects of sunshine duration on wheat growth (Tao et al., 2012). In addition to temperature and sunshine duration, water availability may also exert some effects on wheat growth. Based on the statistical analysis and controlling experiments, some studies have found that increased precipitation or irrigation can slow down the development rate and elongate the growing period of wheat (Lobell et al., 2012; McMaster and Wilhelm, 2003; Nuttonson, 1955), while in another study, precipitation was found to have no significant effects on the heading and flowering dates of wheat (Hu et al., 2005). Moreover, due to the large increase in aerosols released by human activities (such as coal and residue burning), haze weather frequently occurs in winter and spring in China and India (Gupta et al., 2004; Zhang et al., 2012). The severe haze can effectively reduce the receipt of solar radiation and result in lower land surface air temperature (Kaiser and Qian, 2002), which may further act on wheat growth. However, no studies have tried to describe the possible effects of haze on wheat phenology till now. In summary, wheat growth is closely connected with not only climatic factors but also agronomic factors (Abbas et al., 2017; Ahmad et al., 2019; Li et al., 2016; Rezaei et al., 2017; Tariq et al., 2018; Verhulst et al., 2011). Studying wheat phenology dynamics and its relationships with climate and human factors would help scientists and managers to design reasonable strategies to cope with the possibly adverse effects of ongoing climate change on agricultural production.

Additionally, the majority of the above studies were conducted in site scale and limited areas based on discrete ground data. A comprehensive analysis on the effects of environmental factors on wheat phenology at a global scale is still lacking. Compared with limited ground data, satellite data provide us an excellent tool to explore the continuous-space dynamics of wheat phenology at a global scale, as well as their relationships with thermal-moisture conditions (Lobell et al., 2012; White et al., 2009). Therefore, in the present study, we extracted six wheat phenological metrics from satellite data during 1981–2014 and analyzed their relationships with environmental factors at a global scale. The purposes of this study are (1) to analyze what climate factors primarily determine the spatial distribution of wheat phenological events; (2) to assess how temporal pattern of wheat phenology respond to primary climate variables; and (3) to evaluate how haze influences wheat phenology in China and India. Here, we hypothesize that the spatial and temporal patterns of global wheat phenology are primarily controlled by climatic conditions. Haze can indirectly affect wheat phenology in China and India by affecting surface light and heat. It is worth noting that this study does not consider the impact of crop management on wheat phenology.

2. Materials and methods

2.1. Global wheat planting map

In the present study, global wheat distribution was identified based on the Spatial Production Allocation Model 2005 (SPAM2005, http://mapspam.info/global-data), which was released by the International Food Policy Research Institute (You et al., 2014). The SPAM2005 relies on a collection of relevant spatially explicit input data, including crop production statistics, cropland data, biophysical crop "suitability" assessments, population density, as well as any prior knowledge about the spatial distribution of specific crops or crop systems. Its spatial resolution is 5 arc minutes (0.083°, ~10 km). To reduce the effects of other crops and natural vegetation types as much as possible, we focused on the grids where the proportion of wheat is >30% and 40% (Fig. 1) (Lobell et al., 2013; Lobell et al., 2012). However, we only presented the results based on the former in the following sections on account of the larger number of samples and its similar results with the latter. Additionally, to clarify the geographical difference of wheat phenology responses to climate change, we arbitrarily divided the study region into nine major wheat-planting areas, i.e. North America, Europe, Central-West Asia, China, North Africa, South Asia, East Africa, South America, and Australia.

2.2. Remote sensing data and processing

A two-band Enhanced Vegetation Index (EVI2) data product (1981–2014), combined AVHRR (1981–1999) and MODIS (2000–2014) datasets by standardizing AVHRR to the same level of MODIS, was used to calculate the phenological parameters of wheat in 1981 to 2014 in this study. It was previously released by Vegetation Index & Phenology Laboratory at the University of Arizona (https://vip.arizona.edu/viplab_data_explorer.php) and has a spatial resolution of 0.05° and temporal interval of seven days. The discontinuity of the EVI2 values between the two sensors has been solved through a set of robust methods (Didan et al., 2016).

Given the spatial heterogeneity of thermal-moisture condition and socioeconomic status, farming system varies greatly in diverse locations of the world. In cold places and areas with sparse population, farmers usually grow only one crop in a year, while in warm and densely populated areas, farmers may traditionally implement two- or three-crop rotation system, with wheat as one of them. In Northern China Plain, for instance, wheat is usually sown in the last autumn and grows in spring, while corn is cultivated in summer-autumn after harvesting wheat (Fig. 2a). Therefore, for areas where the rotation system is implemented, determination of the corresponding EVI2 profile of wheat from the whole-year EVI2 time series is the precondition step for accurately estimating phenological metrics. In this study, we first chronologically joined the EVI2 time series of all years and removed the poor-quality EVI2 observations in each pixel based on the attached quality data, which are likely to be contaminated by cloud, snow, and ice or affected by the viewing geometry. If poor-quality EVI2 observations account for >30% of the total observations of the year, the EVI2 data of this year

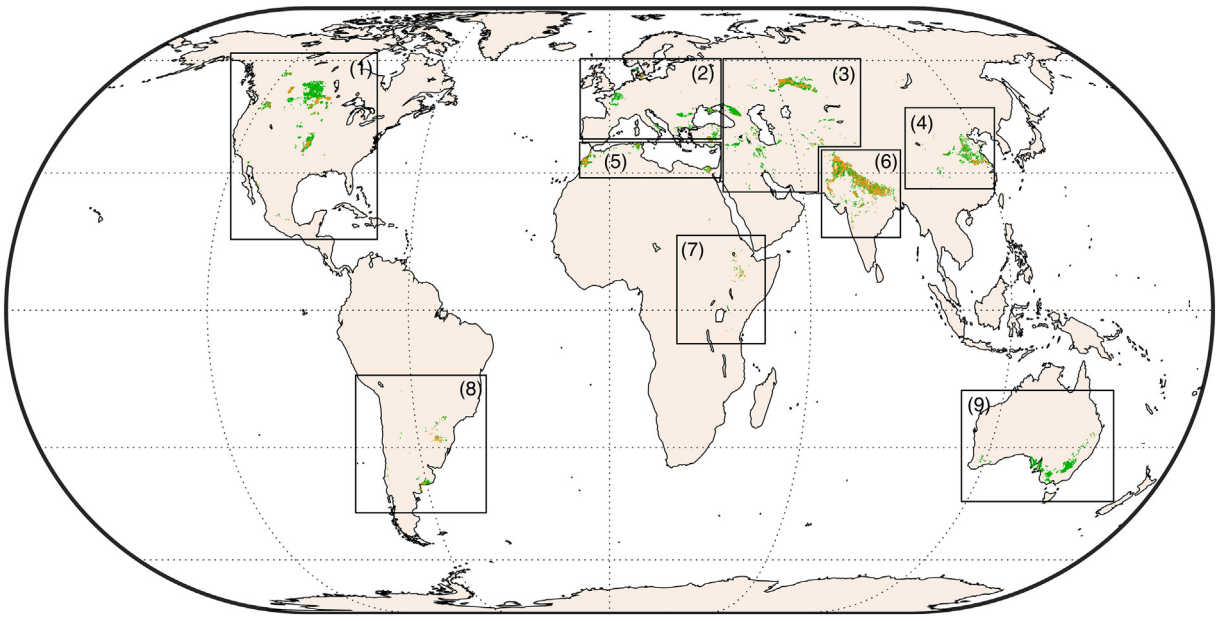

Fig. 1. Global wheat distribution map. The brown areas indicate that the proportion of wheat planted is >40%, while the green parts indicate that the proportion of wheat planted is >30%. 1–9 represent the nine major wheat-planting areas, i.e. North America, Europe, Central-West Asia, China, North Africa, South Asia, East Africa, South America, and Australia.

would be discarded. Next, we smoothed the EVI2 time series and interpolated it into one-day resolution using cubic smooth spline function. Furthermore, with the growing calendar of global wheat summarized by the United States Department of Agriculture (USDA, 1994), the corresponding EVI2 profile of wheat was truncated from the whole-year EVI2 time series. In order to eliminate the effects of other land covers characterized by little seasonal changes, we further removed the pixels with the seasonal amplitude of multiyear average EVI2 time

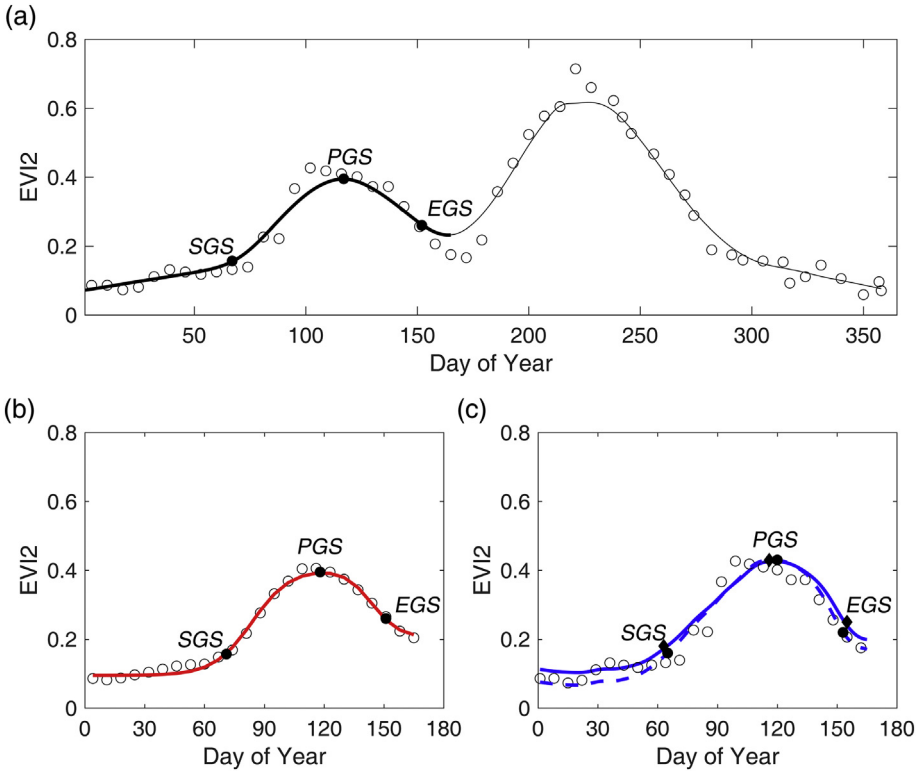

Fig. 2. Diagram of wheat phenology extraction from the two-band Enhanced Vegetation Index (EVI2) time series in China in 1981 by (a) threshold-based method, (b) logistic-based method, and (c) shape-based method. The hollow black point denotes raw EVI2 values. The bold black line in (a) denotes the smoothed growing profile of wheat, while the thin black line denotes the smoothed growing profile of corn. The red line in (b) denotes the fitted EVI2 curve with the double logistic function. The blue solid line in (c) represents the multi-year average EVI2 curve, while the blue dotted line represents the curve scaled from the multiyear average EVI2 curve.

series lower than 0.2. Finally, threshold-, logistic-, and shape-based methods were used to estimate wheat phenological metrics from wheat EVI2 time series in each pixel.

(1) *Threshold-based method*. This method usually defines the critical vegetation growth node as the date when VI reaches a fixed threshold, which has been widely used to estimate phenological parameters from remote sensing data (Lobell et al., 2012; Shen et al., 2014; White et al., 2009). In this study, we defined the growing season start (SGS) and end (EGS) as the dates corresponding to 20% of the amplitude of wheat EVI2 time series in each year, while the growing season peak (PGS) was identified as the corresponding date of the maximum EVI2 value (Fig. 2a).

(2) *Logistic-based method*. Logistic curve is in line with the growth and development of plants and is considered as a perfect model to simulate vegetation growth, as well as track phenological changes from remote sensing data (Beck et al., 2006; Busetto et al., 2010; Fisher et al., 2006; Zhang et al., 2003). The critical growing nodes of vegetation usually correspond well to the turning points of the logistic curve (Fig. 2b). This study used a double logistic function [Eq. (1)] to fit yearly wheat EVI2 time series and computed SGS [Eq. (2)] and EGS [Eq. (3)] based on the maximum curvatures of the fitted curve:

$$EVI2(t) = base + \frac{frange}{1 + e^{mS(S-t)}} - \frac{srange}{1 + e^{mA(A-t)}} \quad (1)$$

$$SGS = S + \frac{\ln\left(2-\sqrt{3}\right)}{mS} \quad (2)$$

$$EGS = A - \frac{\ln\left(2-\sqrt{3}\right)}{mA} \quad (3)$$

Here, *base* denotes the annual minimum EVI2 value; *frange* represents the range from spring minimum EVI2 value to annual maximum EVI2 value; *srange* represents the range from autumn minimum EVI2 value to annual maximum EVI2 value; *mS* and *mA* are the maximum slope values of the fitted curve in spring and autumn, respectively; *S* and *A* are the corresponding dates of *mS* and *mA*, respectively; and PGS was identified as the corresponding date of the maximum EVI2 value in the fitted curve.

(3) *Shape-based method*. This method is first designed by (Sakamoto et al., 2010) to monitor crop phenology in the United States. It assumes that the shape of the VI growth curve (named "shape" curve) is relatively stable for a specific crop in a fixed place. Only geometrical scaling differences exist between the yearly VI curves and the "shape" curve due to local weather conditions and management types. Specifically, in the current study, we determined the "shape" curve of wheat growth in each pixel as the multiyear mean EVI2 time series (Fig. 2c). Then predefined SGS/EGS/PGS was extracted from the "shape" curve by the threshold-based method. The shifted "shape" curve for each year was obtained by fitting yearly EVI2 time series *f(x)* to the "shape" curve *h(x)* [Eq. (4)]:

$$f(x) = xscale \times h(x + tshift) + yscale \quad (4)$$

Here, *x* is the day of year. *xscale*, *tshift*, and *yscale* are scaling parameters that were ascertained based on the smallest root mean square error [RMSE, Eq. (5)] between the shifted "shape" curve and the raw EVI2 time series in each year through the Markov Chain Monte Carlo method.

$$RMSE = \sqrt{\frac{\sum_{i=1}^{n} (P_{EVI2} - R_{EVI2})^2}{n}} \quad (5)$$

Here, P_{EVI2} is the estimated EVI2 value from [Eq. (4)]; R_{EVI2} is the observed EVI2 value; *n* is the number of observations. Yearly SGS/PGS/EGS was then acquired by entering the estimated parameters and the predefined SGS/EGS/PGS into [Eq. (4)].

For the logistic-based and shape-based methods, if the goodness-of-fit value between the fitted and the raw EVI2 time series is lower than 0.8, or the RMSE between the fitted and the raw EVI2 time series is larger than 0.05, wheat phenology parameters calculated in this year would be abandoned because of the bad fitting performance and low credibility of the estimated results. Moreover, to explore the variations of vegetation growth periods, we also defined the period from SGS to EGS as the growing season length (LGS), the period from SGS to PGS as the vegetative period length (LVP), and the period from PGS to EGS as the reproductive period length (LRP).

2.3. Climate and haze data

Two gridded climate data products were used for spatiotemporal pattern analysis of global wheat phenology in this study. There are: (1) the monthly temperature, precipitation, and frost days from Climatic Research Unit TS V4.01 (CRU, https://crudata.uea.ac.uk/cru/data/hrg/); (2) the daily temperature, precipitation, and SW radiation data from the WATCH-Forcing-Data-ERA-Interim data product (WFDEI, http://www.eu-watch.org) (Weedon et al., 2014). Here, the daily SW radiation data were taken as a substitute of sunshine duration to explore the effects of light on wheat phenology (Tao et al., 2014), as the actual gridded sunshine duration data are unavailable at a global scale. Both gridded climate data products have a spatial resolution of 0.5° × 0.5° and time span of 1981–2014. In addition, a satellite-derived yearly $PM_{2.5}$ (atmospheric particulate matter <2.5 μm in diameter) data product (1998–2014) with a spatial resolution of 0.1° × 0.1° was employed to investigate the possible effects of haze on wheat growth, which is provided by the Atmospheric Composition Analysis Group in Dalhousie University (http://fizz.phys.dal.ca/~atmos/martin). To match up with the spatial resolution of climate data and $PM_{2.5}$ data, remotely sensed phenology (0.05° × 0.05°) was upscaled to 0.5° × 0.5° and 0.1° × 0.1° by averaging all the records within a given climate grid, respectively.

2.4. Ground phenology data

The ground-observed greenup/heading/maturity data (1992–2013) at 25 stations in China were used to validate the accuracy of satellite-derived phenological metrics in this study, which were recorded by agrometeorological professionals and provided by China Meteorological Data Service Center (http://data.cma.cn/en). The greenup date is defined as the day when winter wheat resumes to grow and the length of the heart blade reaches 1–2 cm; the heading date is identified as the day when the tip of the ear is exposed from the flag sheath; and the maturity date is characterized as the day when >80% of the grains, husks, and stems turn yellow (China Meteorological Administration, 1993). The observation period varies among different phenophases and stations (Table A.1).

2.5. Analysis

This study first assessed the accuracy of wheat phenology retrieved from three methods by comparing them with ground observations. Pearson's correlation coefficient and mean absolute error (MAE) were calculated between remotely sensed SGS/PGS/EGS and ground-based greenup/heading/maturity date in China. Next, for diagnosing the climatic controls on spatial heterogeneity of global wheat phenology, we obtained the spatial distribution of global wheat phenology (characterized by the multi-year average) with the results based on the best method and analyzed their relationships with spatial pattern of annual mean temperature, annual precipitation, and annual mean SW radiation by means of linear regression analysis.

For temporal pattern analysis, the long-term trends of six wheat phenological parameters and three climate variables were calculated with Theil–Sen estimator, which chooses the median of the slopes of all lines through pairs of two-dimensional sample points (Sen, 1968; Theil, 1950). The Theil–Sen estimator is a robust method for detecting the tendency of temporal series and not affected by extreme outliers. The nonparametric Mann–Kendall test was then used to conduct the significance test of phenological trends at the 0.05 level. To explore the probably spatial difference of phenological temporal variations, we computed the variation trends of wheat phenology and climatic factors over nine primary wheat-planting areas separately. Moreover, we investigated the partial correlations between the interannual fluctuations of six phenological metrics and four climate variables. For SGS, PGS/LVP, EGS/LRP, and LGS, we computed the average temperature, cumulative precipitation, average SW radiation, and average frost days within: (1) the two months before the multiyear average SGS; (2) the period from the multiyear average SGS to the multiyear average PGS; (3) the period from the multiyear average PGS to the multiyear average EGS; and (4) the period from the multiyear average SGS to the multiyear average EGS, respectively. Here, we assumed that climate conditions before one phenological event (such as SGS) have no direct influence on the following phenological events (such as PGS/LVP). And then the sensitivities of six phenological metrics to four climate variables were estimated with Theil–Sen estimator.

Additionally, we analyzed the correlation of $PM_{2.5}$ data and wheat phenology in China and India, where haze is severe (mainly in November–February) (Fig. A.1). Piecewise linear trends of SGS, PGS, EGS, as well as the November–February mean temperature, SW radiation, and frost days during 1981–1997 and 1998–2014 were then obtained and compared.

3. Results

3.1. Phenological comparisons among three methods and ground validation

The accuracies of phenological metrics estimated from threshold-based method, logistic-based method, and shape-based method are very close overall. Specifically, logistic-based SGS is averagely later than threshold-based SGS by about 11.38 days, while logistic-based EGS is slightly earlier than threshold-based EGS by approximately 5.96 days (Fig. A.2). The average difference between shape-based SGS/PGS/EGS and threshold-based SGS/PGS/EGS is limited between 3.28 and 6.53 days. When comparing with ground observations, we found that threshold-based SGS ($R = 0.26$, $P < 0.05$) and logistic-based SGS ($R = 0.29$, $P < 0.05$) are both correlated significantly and positively with ground-observed greenup date (Fig. 3a, d). But they are 12.25 and 14.85 days later than the green dates observed on the ground, respectively. Shape-based SGS has the best estimation accuracy (MAE = 11.63 days) but the weakest ability to reflect spatiotemporal variation of ground-observed greenup date ($R = 0.12$, $P = 0.08$) (Fig. 3g). In comparison, PGS and EGS retrieved from all of the three methods are significantly and positively correlated with ground-observed heading and maturity date, respectively (Fig. 3). The estimated MAE is limited between 5.65 and 6.36 days for PGS and between 4.75 and 5.94 days for EGS, which are far smaller than the estimation error of SGS. Overall, threshold-based method performs a little better than logistic- and shape-based methods in mirroring ground wheat phenology. Therefore, threshold-based phenological metrics were used for the following spatiotemporal pattern analyses of wheat phenology.

3.2. Spatial pattern of wheat phenology and its relationship with climate

Regardless of the wheat-planting areas from 20°N to 20°S, SGS/PGS/EGS occurs gradually earlier from the pole to the equator (Fig. 4). The earliest SGS/PGS/EGS was detected in northern Africa and South Asia, while the latest SGS/PGS/EGS was identified in Argentina and Australia (Fig. A.3). One degree increases from the pole to the equator would lead to SGS/PGS/EGS earlier by 5.7/5.7/5.0 days in the Northern Hemisphere and 5.4/5.4/5.3 days in the Southern Hemisphere. The LGS (limited from 70 to 140 days) exhibits a generally shortening tendency from the pole to the equator, with the shortest located in India, China, and central America. The LVP (25–90 days) is overall a little longer than LRP (20–75 days) across the whole study region.

Further analysis demonstrates that the spatial pattern of SGS/PGS/EGS is significantly and negatively correlated with the spatial pattern of annual mean air temperature, annual mean SW radiation, and annual precipitation in both Northern and Southern Hemisphere ($P < 0.001$), which means that earlier SGS/PGS/EGS mainly occurs in warmer, wetter, and high-SW radiation locations (Fig. 5). The spatial difference of annual mean air temperature, annual mean SW radiation, and annual precipitation can explain >70%, ~45%, and <10% of the spatial variances of SGS/PGS/EGS, respectively. The LGS is also significantly negatively correlated with annual mean temperature, annual precipitation, and annual mean SW radiation ($P < 0.001$), which indicates that the growing period of wheat is shorter in warmer, wetter, and high-SW radiation places (Fig. A.4). The spatial difference of annual mean air temperature, annual precipitation, annual mean SW radiation can explain 20%, 14%, and 12% of the spatial variation of LGS, respectively. The LVP in the Northern Hemisphere also shows a significant negative correlation with all of annual mean air temperature, annual precipitation, annual mean SW radiation ($P < 0.001$), which could explain 38%, 12%, and 25% of the spatial variation of LVP, respectively (Fig. A.4). In comparison, except for the significant correlation between spatial patterns of LRP and annual precipitation in the Southern Hemisphere, no significant correlations were found between LRP and the three climatic factors.

3.3. Trend in wheat phenology and its relationship with climate change

In pixel scale, SGS, PGS, and EGS have significantly advanced in 21.5%, 24.9%, and 32.1% of the study region during 1981–2014, with an average changing rate of −0.53 days/yr, −0.54 days/yr, and −0.45 days/yr, respectively (Fig. 6a, b, Fig. A.5a). Meanwhile, a significant delayed trend of SGS, PGS, and EGS was also detected in 15.6%, 12.8%, and 9.8% of the study region, respectively. Spatially, the advanced SGS/PGS/EGS covers most parts of the study region, while the delayed SGS is mainly located in North America, China, South Asia, and the junction of Kazakhstan and Russia; the delayed PGS is primarily distributed in northern North America, India, and the junction of Kazakhstan and Russia; the delayed EGS was found largely in northern North America. The LGS has significantly shortened by an average of 14.6 days in 20.1% of the study region from 1981 to 2014, compared with 8.7% of the study region showing lengthened growing season (Fig. 6c). The percentage of the study region showing significantly reduced LVP (17.7%) and LRP (17.6%) is also slightly larger than that showing significant extended LVP (12.1%) and LRP (11.7%) (Fig. A.5b, c). The extended LVP primarily concentrates in India and Brazil, while the extended LRP mainly focuses on China, northern North America, and western Australia.

At a regional scale, no significant trend of SGS was observed in Eurasian wheat-planting areas (Fig. A.6a). The PGS in China and EGS in South Asia both present a significantly advanced trend with the changing rate of −0.13 days/yr. In Europe, PGS and EGS have significantly advanced by 0.16 and 0.19 days/yr during 1981–2014, respectively. In North America, however, we detected a significantly delayed trend for all SGS, PGS, and EGS, with the changing rate from 0.23 to 0.29 days/yr. In African wheat planting areas and Southern Hemisphere, almost all SGS, PGS, and EGS have significantly advanced in the past 34 years. The changing rate is limited between −0.08 and −0.38 days/-yr. Regarding the length of growing period, except for a significant lengthened LGS in North Africa (0.06 days/yr), LVP in South Asia (0.1 days/yr) and North Africa (0.13 days/yr), and LRP in Central-West Asia (0.11 days/yr) and North America (0.05 days/yr), we found a

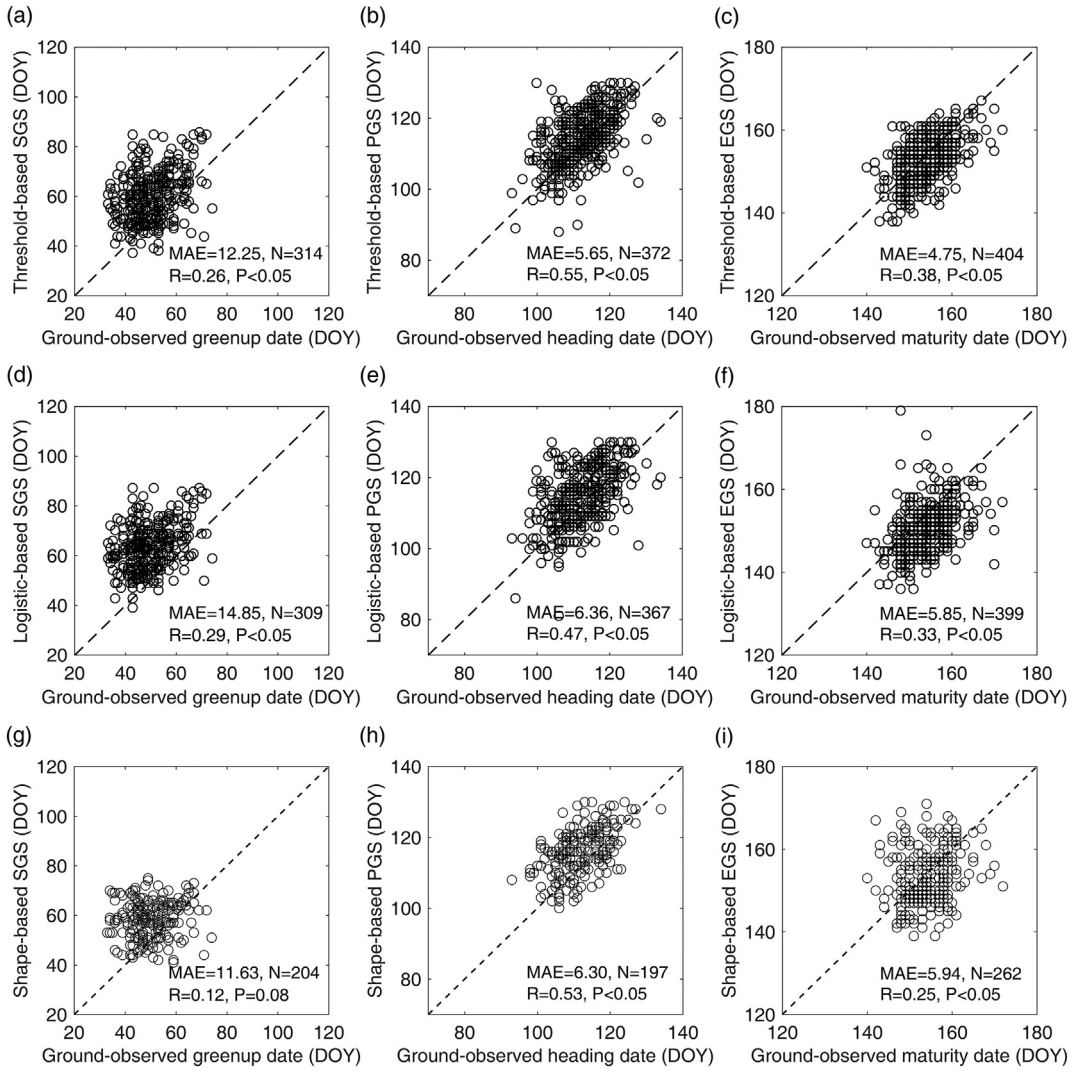

Fig. 3. Comparison between remotely sensed phenology and ground observations. (a)–(c) refer to comparisons between threshold-based growing season start (SGS), peak (PGS), and end (EGS) and ground-observed greenup date, heading date, and maturity date, respectively; (d)–(f) refer to comparisons between logistic-based SGS, PGS, and EGS and ground-observed greenup date, heading date, and maturity date, respectively; (g)–(i) refer to comparisons between shape-based SGS, PGS, and EGS and ground-observed greenup date, heading date, and maturity date, respectively. DOY means the day of year.

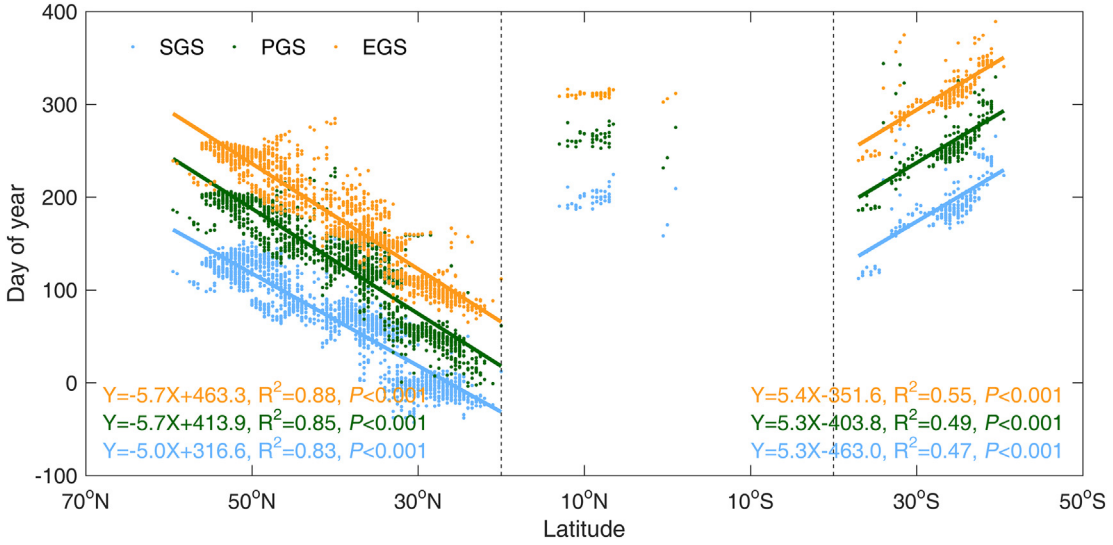

Fig. 4. Relationships between wheat phenology and latitude. To be noted, growing season start (SGS) <0 day of year (SGS takes place in the last year) and growing season end (EGS) >365/366 day of year (EGS appears in the next year) are retained for conveniently analysis due to that growing season peak (PGS) occurs in the current year.

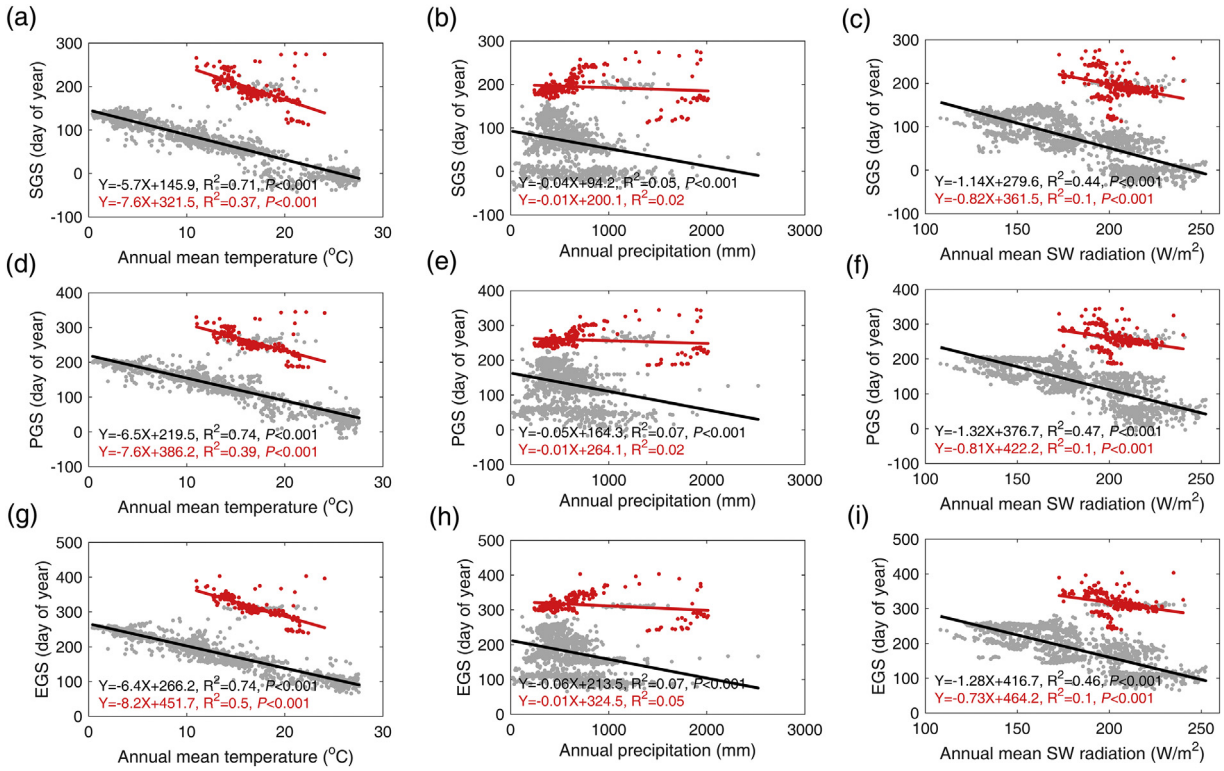

Fig. 5. Relationships between spatial patterns of wheat phenology and climatic factors based on the WATCH-Forcing-Data-ERA-Interim (WFDEI) data in Northern Hemisphere (grey color) and Southern Hemisphere (red color). They are: (a) growing season start (SGS), (d) growing season peak (PGS), (g) growing season end (EGS) vs annual mean temperature; (b) SGS, (e) PGS, (h) EGS vs annual precipitation; (c) SGS, (f) PGS, (i) EGS vs annual mean short-wave (SW) radiation. To be noted, negative SGS values (SGS takes place in the last year) and EGS >365/366 day of year (EGS appears in the next year) are retained for conveniently analysis due to that PGS occurs in the current year.

significantly shortened LGS, or/and LVP, or/and LRP in most wheat-growing areas with a changing rate from −0.08 to −0.36 days/yr (Fig. A.6b).

With regard to the trend in climate change, we found that air temperature in the first two months of SGS to EGS has all significantly increased in China, South Asia, Central-West Asia, Europe and East Africa during 1981–2014, with a changing rate from 0.02 to 0.06 °C/yr (Fig. 7a). A significant increase temperature during the growing season was also detected in South America, Australia and North Africa, which should be primarily attributed to the significant temperature increase in the reproductive period (Fig. 7a). Meanwhile, the precipitation in the first two months of SGS in South Asia (−0.34 mm/yr) and the precipitation in the vegetative period in Australia (−1.1 mm/yr) have decreased significantly, but the precipitation in the vegetative period in North America (1.1 mm/yr) and the precipitation in the whole growing season in East Africa (2.78 mm/yr) showed a significantly increased trend (Fig. 7b). The SW radiation has significantly reduced in China and South Asia and significantly elevated in other wheat-growing regions except North America (Fig. 7c). The frequency of frost in China, South Asia, Central-West Asia, Europe and East Africa has also significantly decreased during the period 1981–2014 (Fig. 7d).

3.4. Interannual variations of wheat phenology in relation to climate changes

The partial correlation analysis results based on CRU data showed that SGS/PGS/EGS is significantly and negatively correlated with previous temperature in 7.1%/8.6%/19.9% of the study region (Fig. 8a). That is, the warmer the previous temperature is, the earlier SGS/PGS/EGS occurs. An increase in previous temperature of 1 °C will cause SGS/PGS/EGS to occur earlier by 1.3/2.4/1.9 days (Fig. A.7a). On the contrary, a significant positive correlation was identified between SGS/PGS/EGS and previous precipitation in a larger proportion of the study region (SGS:6.6%; PGS: 12.9%; EGS: 13.4%), which means that more preseason precipitation would put off the occurrence timing of SGS/PGS/EGS, especially for PGS and EGS. An increase in previous precipitation by 10 mm would delay PGS and EGS by 2.6 and 2.9 days, respectively (Fig. A.7b). Similarly, a significant positive correlation was also detected between SGS/PGS/EGS and previous frost days in 10.6%/9.6%/7.8% of the study region. It means that the frequent frost would delay the occurrence of wheat phenology. SGS/PGS/EGS would be postponed by 3.2/2.3/2.0 days, if the frequency of previous frost events rises by 10 days (Fig. A.7d). The statistical results between SGS/PGS/EGS and previous temperature/precipitation based on WFDEI data are consistent with that based on CRU data, but with larger proportion of samples (SGS:33.1%; PGS: 40.6%; EGS: 31.5%) showing significant negative correlation for temperature (Fig. 8b). Little significant correlations were diagnosed between SGS/PGS/EGS and previous SW radiation in the study region.

Moreover, we detected a predominant significant negative correlation between LGS/SPL/PEL and in-season mean temperature (CRU: 15.0%/9.1%/9.8%; WFDEI: 11.9%/11.7%/8.8%). An increase in previous temperature of 1 °C will shorten the duration of LGS/SPL/PEL by 1.0/0.6/0.4 days (Fig. A.7a). Simultaneously, LGS/SPL/PEL was also correlated negatively and positively with in-season frost days in 9.1%/11.3%/5.1% of study regions, which indicates that frequent frost could also cause a shorter growing season of wheat. Little significant correlations were found between LGS/SPL/PEL and precipitation/short-wave radiation (Fig. 8).

3.5. Effects of haze on wheat phenology in China and India

A significant positive correlation ($P < 0.1$) was detected between SGS/PGS/EGS and $PM_{2.5}$ in China (Fig. 9a), which means that higher

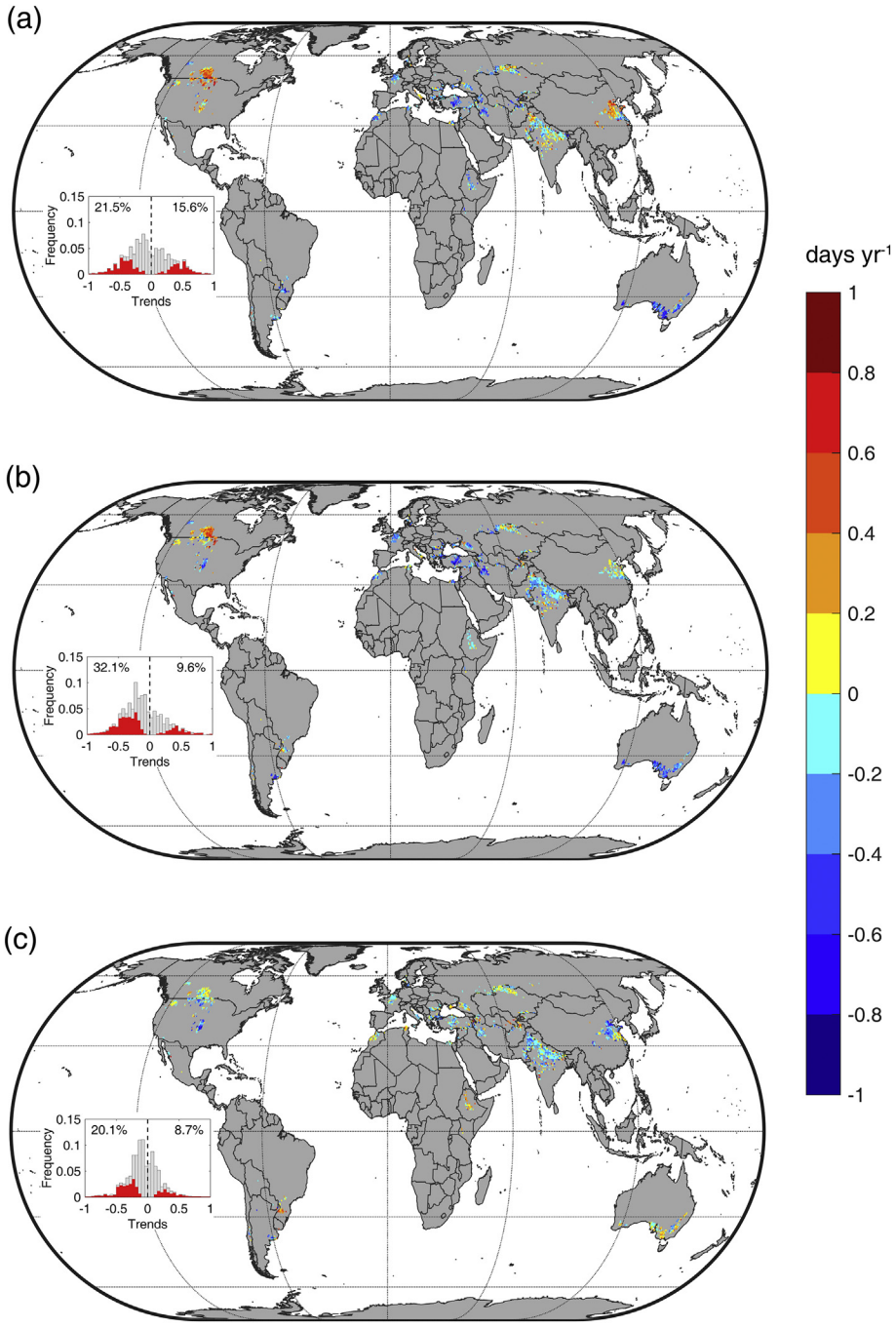

Fig. 6. Spatial distribution of variation trends of (a) growing season start (SGS), (b) growing season end (EGS), (c) growing season length (LGS) during 1981–2014. The embedded plot represents the frequency of trends. The value in the upper left corner denotes the proportion of pixels showing significantly advanced/shortened trend to the total pixels; the value in the upper right corner denotes the proportion of pixels showing significant delayed/elongated trend to the total pixels.

$PM_{2.5}$ could postpone the whole growth period of wheat in China. On the contrary, a significant negative correlation ($P < 0.05$) was identified between SGS and $PM_{2.5}$ in India (Fig. 9b), which indicates that wheat greens up earlier in years with higher $PM_{2.5}$. Besides, we found that SGS/PGS/EGS in China showed a non-significant advanced trend from 1981 to 1997 but a significant delayed trend from 1998 to 2014 (Fig. A.8a–c), while SGS in India has significantly delayed during 1981–1997 but non-significantly advanced during 1998–2014 (Fig. A.8d–f). $PM_{2.5}$ was found to have significantly increased since 1998 in both China and India (Fig. 10a, e). Meanwhile, in the two regions, we detected a reversed trend of temperature and frost days between 1981–1997 and 1998–2014 and an accelerated decline of SW radiation since 1998 (Fig. 10).

4. Discussion

To date, a large amount of research has focused on exploring the effects of global and regional climate change on wheat phenology (Estrella et al., 2007; Hu et al., 2005; Liu et al., 2018; Xiao et al., 2015). However, only a few have tried to detect the spatial pattern of wheat phenology and its climate control (Tao et al., 2012). Revealing the spatial pattern of global wheat phenology is critical to estimating the spatial heterogeneity of wheat production. This study revealed an advance trend of wheat phenological events and a shortening tendency of wheat growth period lengths from the pole to the equator, which are primarily determined by the spatial variations of air temperature (Tao et al., 2012). That is because winter-spring temperature gradually

Fig. 7. Variation trends of (a) temperature, (b) precipitation, (c) short-wave (SW) radiation, and (d) frost days during four periods in nine wheat-growing areas. * denotes significance level $P < 0.1$; ** denotes significance level $P < 0.05$. Here, the temperature, precipitation, and SW radiation data are from the WATCH-Forcing-Data-ERA-Interim (WFDEI) data, while the frost data is from the Climatic Research Unit TS V4.01 (CRU) data. SGS: growing season start; PGS: growing season peak; and EGS: growing season end.

increases from high latitude to low latitude. In the low-latitude wheat-growing areas, the earlier satisfaction of thermal requirements makes wheat green up earlier. The latitudinal gradient of wheat phenology maybe has little to do with wheat types (namely winter wheat and spring wheat). Because winter wheat covers the majority (>75%) of the world wheat-growing areas, while spring wheat only dominates

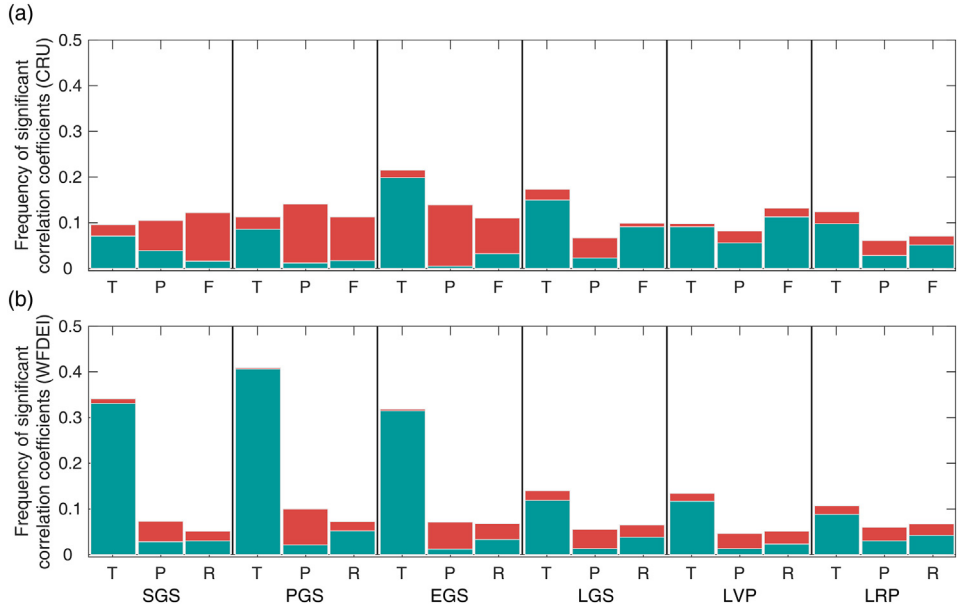
(a)
Frequency of significant correlation coefficients (CRU)
(b)
Frequency of significant correlation coefficients (WFDEI)
T P F T P F T P F T P F T P F T P F
T P R T P R T P R T P R T P R T P R
SGS
PGS
EGS
LGS
LVP
LRP

Fig. 8. Frequency of significant partial correlation coefficients between wheat phenology and climatic factors for (a) the Climatic Research Unit TS V4.01 (CRU) data and (b) the WATCH-Forcing-Data-ERA-Interim (WFDEI) data, respectively. T denotes temperature; F denotes frost days; P denotes precipitation; R denotes short-wave radiation. SGS: growing season start; PGS: growing season peak; EGS: growing season end; LGS: growing season length; LVP: vegetative period length; LRP: reproductive period length.

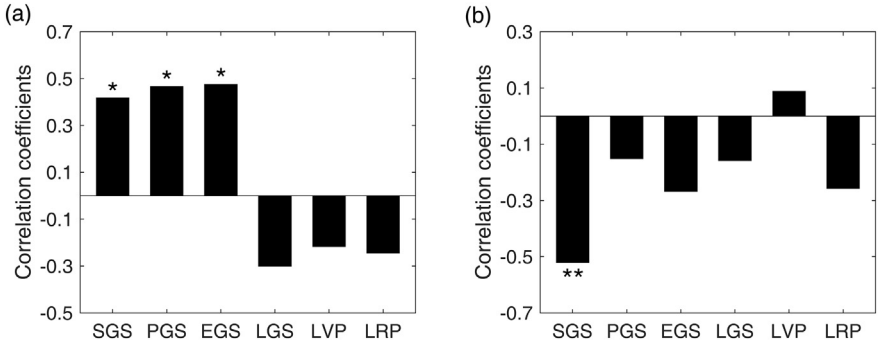

Fig. 9. Correlations between wheat phenology and $PM_{2.5}$ in (a) China and (b) India. * denotes significance level $P < 0.1$; ** denotes significance level $P < 0.05$. SGS: growing season start; PGS: growing season peak; EGS: growing season end; LGS: growing season length; LVP: vegetative period length; LRP: reproductive period length.

<25% of the world wheat-growing areas (primarily in northern North America, Russia and Kazakhstan) (USDA, 1994). The differences of regression coefficients of wheat phenology and climatic factors between Northern Hemisphere and Southern Hemisphere maybe mainly stem from the contrasting sample sizes and spatial differences of climate conditions. Due to the vast wheat-growing area, sample size and spatial difference of climate conditions in Northern Hemisphere are greatly larger than that in Southern Hemisphere.

For the long-term phenological trends, we detected a significantly advanced trend of SGS/PGS/EGS and a significantly shortened trend of LGS/LVP/LRP in a large proportion of the study region during 1981–2014. Based on numerous ground-observed data, a similar advanced trend of post-dormancy phenological events and a shortened vegetative and reproductive period of wheat have also been extensively diagnosed by previous studies in China (Tao et al., 2006; Tao et al., 2012; Xiao et al., 2013), Germany (Estrella et al., 2007), Australia and Argentina (Sadras and Monzon, 2006) since 1950s. The more widely shifted forward of EGS may suggest a stronger effect of climate change on EGS than that on SGS/PGS, which is consistent with the study carried out in North China Plain by Xiao et al. (2013). At the regional scale, the variation trends of wheat vary among different wheat-planting areas. The SGS, PGS, and EGS in North America all present a significantly delayed trend from 1981 to 2014, which may be induced together by the decreased temperature and insolation, as well as the increased precipitation and frost days in previous periods (Fig. 7). Because of the reduced temperature, the thermal conditions that are suitable for vegetation growth are delayed. Earlier growth may induce wheat to be damaged by more frequent frost (Fuller et al., 2007). Besides, the increased precipitation may also delay the wheat growth in North America to some extent. In other eight wheat-planting areas, however, a dominant advanced trend of SGS/PGS/EGS and a dominant shortened trend of LGS/LVP/LRP were diagnosed, which could be primarily attributed to the consistent increased temperature and decreased frost days, as well as the increase of SW radiation in most regions apart from China and South Asia (Fig. 7). The increased temperature signifies a fast effective temperature accumulation and thus leads to an earlier growth of wheat under enough light capture (Porter and Gawith, 1999). In addition, LRP variations were found to largely contribute to LGS variations in this study, which is different from the larger contribution of the time from sowing to flowering to growing season length variations revealed in Australia and Argentina (Sadras and Monzon, 2006).

Regards to the interannual fluctuations of wheat phenology, we identified a dominant significant negative correlation between SGS/PGS/EGS and previous temperature, as well as a dominant significant negative correlation between LGS/SPL/PEL and in-season temperature. This finding indicates that higher temperature would facilitate the full growth period of wheat to occur earlier and shorten the duration of each growth period. That's because high temperature can speed up

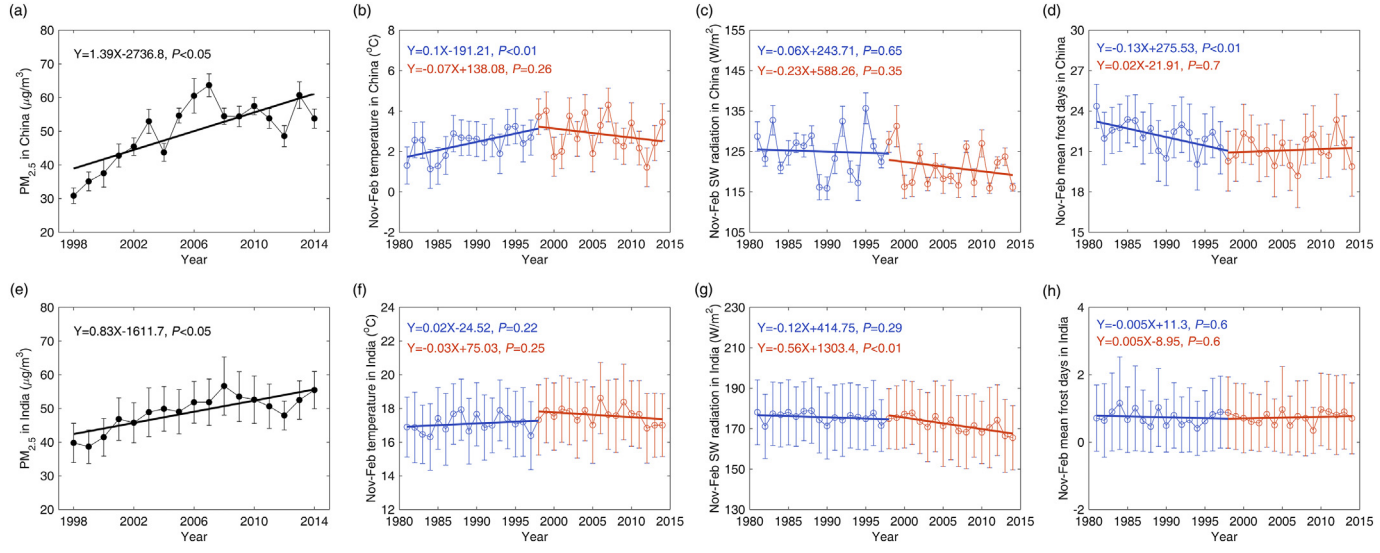

Fig. 10. Variation trends of $PM_{2.5}$ (1981–1997), November–December mean temperature, November–December mean short-wave (SW) radiation, and November–December mean frost days for 1981–1997 and 1998–2014 in (a–d) China and (e–h) India. Here, the temperature, precipitation, and SW radiation data are from the WATCH-Forcing-Data-ERA-Interim (WFDEI) data, while the frost data is from the Climatic Research Unit TS V4.01 (CRU) data. The bar denotes standard deviation.

wheat growth and therefore a short time span is needed to satisfy the heat accumulation requirements for reaching the next phenological stage, which finally lead to a shorter growing period (Tao et al., 2012). Meanwhile, a predominant significant positive correlation between SGS/PGS/EGS and previous precipitation and between SGS/PGS/EGS and previous frost days was also detected in the study region. It indicates that more precipitation and frost days in the preseason would postpone the occurrence timing of SGS/PGS/EGS and extend the growing period of wheat. The positive effect (especially for PGS/EGS) of water availability has also been unveiled by McMaster and Wilhelm (2003) through in-situ controlling experiments in two winter-wheat-planting locations of America, which may be primarily attributed to the fact that later growth stages occur at considerably higher temperatures when evaporative demand is high, which would cause greater water stress and higher plant temperatures (McMaster and Wilhelm, 2003). Frost could also interrupt wheat growth by causing dehydration of cells and destroying metabolic processes (Zheng et al., 2012), especially for SGS when low temperature events frequently appear. Moreover, we also identified a dominant negative correlation between PGS and short-wave radiation with WFDEI data, as the vegetative growth stage of wheat is also susceptive to light variations. Overall, wheat phenology may theoretically depend on the interactive effects of previous temperature, precipitation, light, and frost, though with different degrees of influence in different phenophases. Nevertheless, we still emphasize the stronger role of temperature in modulating most wheat phenophases than precipitation, light and frost (Liu et al., 2018).

Due to the large amount of industrial and agricultural aerosol emissions, severe haze weather often occurs in winter and spring in China and India. A direct consequence of frequent haze weather is the reduction of light capture, which has led to a decreased temperature and a reduced sunshine duration in the two regions (Kaiser and Qian, 2002; Ramanathan et al., 2001). Though haze weather has similar influence on local climate, an opposite effect of haze on wheat phenology was identified in China and India in the current study. Namely, a stronger haze weather could put off the growth process of wheat in China but advance wheat phenophases in India. For wheat in China, the temperature reduction induced by haze weather would cause the vernalization process to be completed early. But the continuous low temperature and insufficient light acquisition after vernalization are unfavorable to wheat growth and thus postpone the entire wheat growth process until the heat and light requirements are reached (Porter and Gawith, 1999). Because enough effective temperature accumulation and suitable sunshine duration are necessary to the greenup of wheat in the next spring (Davidson and Campbell, 1983; Miglietta, 1989). In India, however, winter mean temperature is still >16 °C. The lower temperature induced by the increased haze weather would also be helpful to the accomplishment of vernalization process in advance (Wang et al., 2015). But unlike in China, the warmer temperature after vernalization is favorable to wheat growth. Thus, wheat develops immediately after vernalization and all growth stages move forward. To be noted, we didn't consider the impacts of haze components on wheat biochemical process because of its complexity (Zhang et al., 2012).

However, expect for natural factors, wheat growth progress is also unavoidable to be influenced by human decision-making, such as sowing earlier or later, the choice of varieties with shorter or longer growing season, and the introduction of new cultivars with stronger tolerance of heat or drought stress (He et al., 2015; Liu et al., 2018; Wang et al., 2013). All of them may incur a sharp shift of wheat phenology, which is hard to be distinguished from the effects of environmental factors even if some agriculture management data is available in global scale. Another possible uncertainty of this study may stem from the selection of study region (dominated by at least 30% and 40% wheat), there are still 60%–70% parts mixed other vegetation types or non-vegetation types, which might have great contributions to the finally estimated wheat phenology. There are few pixels fully covered by wheat. Even though we choose pixels with a wheat planting ratio >70% or 80%, only a very small number of areas (<100 pixels) would be incorporated. Therefore, as done in other studies (Lobell et al., 2013; Lobell et al., 2012), we had to select pixels with a wheat planting ratio of at least 30% and 40% in this study.

Nevertheless, we believe our study has great meaningful for understanding wheat phenology responses to environment factors and could provide useful information for wheat management. The occurrence timing of phenological events and the length of the growing period is of crucial importance to wheat yields (Rosenzweig and Tubiello, 1996; Tao et al., 2006). In the context of rising temperatures in the future, the occurrence of wheat phenology will be earlier and the length of wheat growth will be further shortened (Yang et al., 2014). Meanwhile, the frequency and intensity of heat waves and droughts will continue to increase, which may further threaten wheat productions (Battisti and Naylor, 2009). Therefore, new cultivars with heat tolerance and longer growing season should be developed to deal with the ongoing climate change for securing high yields.

5. Conclusion

Remote sensing data provide us an excellent tool to study wheat growth status in global scale. With the reliable phenology estimated from EVI2 data, this study identified a dominant control of air temperature on spatial distribution and temporal variations of wheat phenology, while precipitation and SW radiation exerted only significant effects on wheat phenology. Frequent frost could also postpone the occurrence timing of wheat phenology, especially for SGS. Unexpectedly, the decreased temperature as a result of severe haze weather in China has counteracted the advancing trend of wheat phenology induced by global warming to some extent. However, the decreased temperature resulted from severe haze weathers in India has further advanced the occurrence timing of wheat phenology through prompting vernalization.

Declarations of interest

None.

Acknowledgements

This study was supported by the National Natural Science Foundation of China (41771371), Projects of International Cooperation and Exchanges NSFC (61661136006002), and the National High-Resolution Earth Observation Project (11-Y20A16-9001-17/18). We would like to thank the Vegetation Index and Phenology Lab., University of Arizona for providing high-quality EVI2 data.

Appendix A. Supplementary data

Supplementary data to this article can be found online at https://doi.org/10.1016/j.scitotenv.2019.01.394.

References

Abbas, T., Rizwan, M., Ali, S., Zia-ur-Rehman, M., Qayyum, M.F., Abbas, F., et al., 2017. Effect of biochar on cadmium bioavailability and uptake in wheat (*Triticum aestivum L.*) grown in a soil with aged contamination. Ecotoxicol. Environ. Saf. 140, 37–47.

Ahmad, S., Abbas, G., Ahmed, M., Fatima, Z., Anjum, M.A., Rasul, G., et al., 2019. Climate warming and management impact on the change of phenology of the rice-wheat cropping system in Punjab, Pakistan. Field Crop Res. 230, 46–61.

Asseng, S., Ewert, F., Martre, P., Rötter, R.P., Lobell, D., Cammarano, D., et al., 2015. Rising temperatures reduce global wheat production. Nat. Clim. Chang. 5, 143–147.

Battisti, D.S., Naylor, R.L., 2009. Historical warnings of future food insecurity with unprecedented seasonal heat. Science 323, 240–244.

Beck, P.S.A., Atzberger, C., Høgda, K.A., Johansen, B., Skidmore, A.K., 2006. Improved monitoring of vegetation dynamics at very high latitudes: a new method using MODIS NDVI. Remote Sens. Environ. 100, 321–334.

Busetto, L., Colombo, R., Migliavacca, M., Cremonese, E., Meroni, M., Galvagno, M., et al., 2010. Remote sensing of larch phenological cycle and analysis of relationships with climate in the Alpine region. Glob. Chang. Biol. 16, 2504–2517.

China Meteorological Administration, 1993. Observation Criterion of Agricultural Meteorology. China Meteorological Press, Beijing.
Cleland, E.E., Chiariello, N.R., Loarie, S.R., Mooney, H.A., Field, C.B., 2006. Diverse responses of phenology to global changes in a grassland ecosystem. Proc. Natl. Acad. Sci. 103, 13740–13744.
Davidson, H., Campbell, C., 1983. The effect of temperature, moisture and nitrogen on the rate of development of spring wheat as measured by degree days. Can. J. Plant Sci. 63, 833–846.
Didan, K., Barreto, A., Miura, T., Tsend-Ayush, J., Zhang, X., Friedl, M., et al., 2016. Multi-sensor Vegetation Index and Phenology Earth Science Data Records: Algorithm Theoretical Basis Document and User Guide Version 4.0.
Estrella, N., Sparks, T.H., Menzel, A., 2007. Trends and temperature response in the phenology of crops in Germany. Glob. Chang. Biol. 13, 1737–1747.
Estrella, N., Sparks, T.H., Menzel, A., 2009. Effects of temperature, phase type and timing, location, and human density on plant phenological responses in Europe. Clim. Res. 39, 235–248.
Fisher, J.I., Mustard, J.F., Vadeboncoeur, M.A., 2006. Green leaf phenology at Landsat resolution: scaling from the field to the satellite. Remote Sens. Environ. 100, 265–279.
Fuller, M.P., Fuller, A.M., Kaniouras, S., Christophers, J., Fredericks, T., 2007. The freezing characteristics of wheat at ear emergence. Eur. J. Agron. 26, 435–441.
Gupta, P.K., Sahai, S., Singh, N., Dixit, C.K., Singh, D.P., Sharma, C., et al., 2004. Residue burning in rice-wheat cropping system: causes and implications. Curr. Sci. 87, 1713–1717.
He, L., Asseng, S., Zhao, G., Wu, D., Yang, X., Zhuang, W., et al., 2015. Impacts of recent climate warming, cultivar changes, and crop management on winter wheat phenology across the Loess Plateau of China. Agric. For. Meteorol. 200, 135–143.
Hu, Q., Weiss, A., Feng, S., Baenziger, P.S., 2005. Earlier winter wheat heading dates and warmer spring in the U.S. Great Plains. Agric. For. Meteorol. 135, 284–290.
Kaiser, D.P., Qian, Y., 2002. Decreasing trends in sunshine duration over China for 1954–1998: indication of increased haze pollution? Geophys. Res. Lett. 29 (38-1-38-4).
Li, K.N., Yang, X.G., Tian, H.Q., Pan, S.F., Liu, Z.J., 2016. Lu S. Effects of changing climate and cultivar on the phenology and yield of winter wheat in the North China Plain. Int. J. Biometeorol. 60, 21–32.
Liu, Y.J., Chen, Q.M., Ge, Q.S., Dai, J.H., Qin, Y., Dai, L., et al., 2018. Modelling the impacts of climate change and crop management on phenological trends of spring and winter wheat in China. Agric. For. Meteorol. 248, 518–526.
Lobell, D.B., Sibley, A., Ivan Ortiz-Monasterio, J., 2012. Extreme heat effects on wheat senescence in India. Nat. Clim. Chang. 2, 186–189.
Lobell, D.B., Ortiz-Monasterio, J.I., Sibley, A.M., Sohu, V.S., 2013. Satellite detection of earlier wheat sowing in India and implications for yield trends. Agric. Syst. 115, 137–143.
Lokupitiya, E., Denning, S., Paustian, K., Baker, I., Schaefer, K., Verma, S., et al., 2009. Incorporation of crop phenology in Simple Biosphere Model (SiBcrop) to improve land-atmosphere carbon exchanges from croplands. Biogeosciences 6, 969–986.
Matuszko, D., 2012. Influence of cloudiness on sunshine duration. Int. J. Climatol. 32, 1527–1536.
McMaster, G., Wilhelm, W., 2003. Phenological responses of wheat and barley to water and temperature: improving simulation models. J. Agric. Sci. 141, 129–147.
Miglietta, F., 1989. Effect of photoperiod and temperature on leaf initiation rates in wheat (*Triticum spp.*). Field Crop Res. 21, 121–130.
Nuttonson, M.Y., 1955. Wheat-Climate Relationships and the Use of Phenology in Ascertaining the Thermal and Photo-thermal Requirements of Wheat. American Institute of Crop Ecology, Washington.
Penuelas, J., Rutishauser, T., Filella, I., 2009. Phenology feedbacks on climate change. Science 324, 887–888.
Piao, S., Ciais, P., Friedlingstein, P., Peylin, P., Reichstein, M., Luyssaert, S., et al., 2008. Net carbon dioxide losses of northern ecosystems in response to autumn warming. Nature 451, 49–52.
Porter, J.R., Gawith, M., 1999. Temperatures and the growth and development of wheat: a review. Eur. J. Agron. 10, 23–36.
Ramanathan, V., Crutzen, P.J., Lelieveld, J., Mitra, A., Althausen, D., Anderson, J., et al., 2001. Indian Ocean experiment: an integrated analysis of the climate forcing and effects of the great Indo-Asian haze. J. Geophys. Res.-Atmos. 106, 28371–28398.
Ramankutty, N., Foley, J.A., 1998. Characterizing patterns of global land use: an analysis of global croplands data. Glob. Biogeochem. Cycles 12, 667–685.
Rezaei, E.E., Siebert, S., Ewert, F., 2017. Climate and management interaction cause diverse crop phenology trends. Agric. For. Meteorol. 233, 55–70.
Richardson, A.D., Keenan, T.F., Migliavacca, M., Ryu, Y., Sonnentag, O., Toomey, M., 2013. Climate change, phenology, and phenological control of vegetation feedbacks to the climate system. Agric. For. Meteorol. 169, 156–173.
Rosenzweig, C., Tubiello, F.N., 1996. Effects of changes in minimum and maximum temperature on wheat yields in the central US a simulation study. Agric. For. Meteorol. 80, 215–230.
Sadras, V.O., Monzon, J.P., 2006. Modelled wheat phenology captures rising temperature trends: shortened time to flowering and maturity in Australia and Argentina. Field Crop Res. 99, 136–146.
Sakamoto, T., Wardlow, B.D., Gitelson, A.A., Verma, S.B., Suyker, A.E., Arkebauer, T.J., 2010. A two-step filtering approach for detecting maize and soybean phenology with time-series MODIS data. Remote Sens. Environ. 114, 2146–2159.
Sen, P.K., 1968. Estimates of the regression coefficient based on Kendall's tau. J. Am. Stat. Assoc. 63, 1379–1389.
Shen, M., Zhang, G., Cong, N., Wang, S., Kong, W., Piao, S., 2014. Increasing altitudinal gradient of spring vegetation phenology during the last decade on the Qinghai–Tibetan Plateau. Agric. For. Meteorol. 189-190, 71–80.
Siebert, S., Ewert, F., 2012. Spatio-temporal patterns of phenological development in Germany in relation to temperature and day length. Agric. For. Meteorol. 152, 44–57.
Tao, F., Yokozawa, M., Xu, Y., Hayashi, Y., Zhang, Z., 2006. Climate changes and trends in phenology and yields of field crops in China, 1981–2000. Agric. For. Meteorol. 138, 82–92.
Tao, F., Zhang, S., Zhang, Z., 2012. Spatiotemporal changes of wheat phenology in China under the effects of temperature, day length and cultivar thermal characteristics. Eur. J. Agron. 43, 201–212.
Tao, F.L., Zhang, Z., Xiao, D.P., Zhang, S., Rotter, R.P., Shi, W.J., et al., 2014. Responses of wheat growth and yield to climate change in different climate zones of China, 1981-2009. Agric. For. Meteorol. 189, 91–104.
Tariq, M.J., Shah, M.K.N., Hassan, M.U., Sajjad, M., Jamil, M., Ali, N., et al., 2018. Prevelance of higher glutenin variation in synthetic wheat germplasm. J. Anim. Plant Sci. 28, 568–575.
Theil, H., 1950. A Rank-invariant Method of Linear and Polynomial Regression Analysis, I, II, and III. 58. Nederlandsche Akad. van Wetenschappen Proc, pp. 386–392.
USDA, 1994. Major world crop areas and climatic profiles. Agricultural Handbook. 664, p. 279.
Verhulst, N., Govaerts, B., Nelissen, V., Sayre, K.D., Crossa, J., Raes, D., et al., 2011. The effect of tillage, crop rotation and residue management on maize and wheat growth and development evaluated with an optical sensor. Field Crop Res. 120, 58–67.
Wang, J., Wang, E., Feng, L., Yin, H., Yu, W., 2013. Phenological trends of winter wheat in response to varietal and temperature changes in the North China Plain. Field Crop Res. 144, 135–144.
Wang, B., Li Liu, D., Asseng, S., Macadam, I., Yu, Q., 2015. Impact of climate change on wheat flowering time in eastern Australia. Agric. For. Meteorol. 209, 11–21.
Weedon, G.P., Balsamo, G., Bellouin, N., Gomes, S., Best, M.J., Viterbo, P., 2014. The WFDEI meteorological forcing data set: WATCH forcing data methodology applied to ERA-interim reanalysis data. Water Resour. Res. 50, 7505–7514.
White, M.A., De Beurs, K.M., Didan, K., Inouye, D.W., Richardson, A.D., Jensen, O.P., et al., 2009. Intercomparison, interpretation, and assessment of spring phenology in North America estimated from remote sensing for 1982–2006. Glob. Chang. Biol. 15, 2335–2359.
Xiao, D., Tao, F., Liu, Y., Shi, W., Wang, M., Liu, F., et al., 2013. Observed changes in winter wheat phenology in the North China Plain for 1981–2009. Int. J. Biometeorol. 57, 275–285.
Xiao, D., Moiwo, J.P., Tao, F., Yang, Y., Shen, Y., Xu, Q., et al., 2015. Spatiotemporal variability of winter wheat phenology in response to weather and climate variability in China. Mitig. Adapt. Strateg. Glob. Chang. 20, 1191–1202.
Yang, Y., Li Liu, D., Anwar, M.R., Zuo, H., Yang, Y., 2014. Impact of future climate change on wheat production in relation to plant-available water capacity in a semiaridenvironment. Theor. Appl. Climatol. 115, 391–410.
You, L.Z., Wood, S., Wood-Sichra, U., Wu, W.B., 2014. Generating global crop distribution maps: from census to grid. Agric. Syst. 127, 53–60.
Zhang, X., Friedl, M.A., Schaaf, C.B., Strahler, A.H., Hodges, J.C.F., Gao, F., et al., 2003. Monitoring vegetation phenology using MODIS. Remote Sens. Environ. 84, 471–475.
Zhang, X.Y., Wang, Y.Q., Niu, T., Zhang, X.C., Gong, S.L., Zhang, Y.M., et al., 2012. Atmospheric aerosol compositions in China: spatial/temporal variability, chemical signature, regional haze distribution and comparisons with global aerosols. Atmos. Chem. Phys. 12, 779–799.
Zheng, B., Chenu, K., Fernanda Dreccer, M., Chapman, S.C., 2012. Breeding for the future: what are the potential impacts of future frost and heat events on sowing and flowering time requirements for Australian bread wheat (*Triticum aestivium*) varieties? Glob. Chang. Biol. 18, 2899–2914.